applied sciences

MDPI

Article

Diode-Pumped Solid-State Q-Switched Laser with Rhenium Diselenide as Saturable Absorber

Chun Li [1,2,3], Yuxin Leng [2,*] and Jinjin Huo [4]

1 School of Physics Science and Engineering, Tongji University, Shanghai 200092, China; lichunqingchen@126.com
2 State Key Laboratory of High Field Laser Physics, Shanghai Institute of Optics and Fine Mechanics, Chinese Academy of Sciences, Shanghai 201800, China
3 University of Chinese Academy of Sciences, Beijing 100049, China
4 Jingjiang Photoelectric Technology Co. Ltd., Jinan 250000, China; jingjiang_opt@163.com
* Correspondence: lengyuxin@mail.siom.ac.cn

Received: 7 August 2018; Accepted: 20 September 2018; Published: 28 September 2018

Abstract: We report a solid-state passively Q-switched Nd:YVO_4 laser adopting rhenium diselenide ($ReSe_2$) as saturable absorber (SA) materials. $ReSe_2$ belongs to a type of transition metal dichalcogenides (TMDs) materials and it has the weak-layered dependent feature beneficial for the preparation of few-layer materials. The few-layer $ReSe_2$ was prepared by ultrasonic exfoliation method. Using a power-dependent transmission experiment, its modulation depth and saturation intensity were measured to be 1.89% and 6.37 MW/cm^2. Pumped by diode laser and based on few-layer $ReSe_2$ SA, the Q-switched Nd:YVO_4 laser obtained the shortest Q-switched pulse width of 682 ns with the highest repetition rate of 84.16 kHz. The maximum average output power was 125 mW with the slope efficiency of 17.27%. Our experiment, to the best of our knowledge, is the first demonstration that used $ReSe_2$ as SA materials in an all-solid-state laser. The results show that the few-layer $ReSe_2$ owns the nonlinear saturable absorption properties and it has the capacity to act as SA in an all-solid-state laser.

Keywords: all-solid-state laser; $ReSe_2$ SA; Q-switched laser

1. Introduction

Few-layer materials are of great importance to researches and applications due to their unique optical and electronic characteristics. Current researches on few-layer materials are principally focused on graphene, insulating hexagonal boron nitride (hBN), topological insulators (TIs), black phosphorus (BP), and transition metal dichalcogenides (TMDs) [1–6]. Among these materials, TMDs are a large family, which exhibits a variety of photo-electric properties and offers a wide range of applications in broad research fields [5,6].

TMDs include some metals, various semiconductors, as well as superconductors. Over years of development, studies of TMDs have mainly concentrated on MoS_2, $MoSe_2$, WS_2, and WSe_2 [7–9]. They have a changed characteristic (such as electronic structure, band gap) with their different layer thickness, owing to interlayer interactions and the variations of screening. While some TMDs have different transformation characteristics when the structure is changed from bulk to single or few-layer. Reports show that both SnS_2 and $SnSe_2$ (one type of TMDs) are layer-independent on in-plane lattice parameters, interlayer distances, and binding energies [10,11]. In addition, the $ReSe_2$ class also has different transformation characteristics with the change of the number of layers.

$ReSe_2$, a new member of semiconductor TMDs, owns the distorted 1T structure, compared with the typical 2H-shaped MoS_2 class of TMDs [12]. In their in-plane, Re atoms arrange in linked Re_4 "diamond" shapes along the b [010] direction. These Re_4 'diamonds' are coplanar and are

coupled with one another to form a one-dimensional clustering pattern of 'diamond chains' [13]. Its distorted 1T structure results in the weaker interlayer coupling action [12–17]. Further, $ReSe_2$ behaves as electronically and vibrationally decoupled monolayers [15,16]. The weaker interlayer coupling action makes $ReSe_2$ weak-layered dependence. Due to the distorted 1T structure, $ReSe_2$ has a low-symmetry lattice characteristic that is similar to ReS_2 and BP [18]. In different directions of the in-plane structure of $ReSe_2$, there are significant differences in properties, including phonon behavior, magnetic characteristics, transport properties, and so on [19]. Therefore, this material has a larger variation in physical, chemical, optical, and electrical properties, and it has great potential in applications [20–26].

With the rapid development of the material applications, one of the significant applications of the few-layer TMDs are to be used as SA. Such as MoS_2 have been widely studied in the field of fiber laser and all-solid-state laser [27,28]. Recently, SnS_2 and $SnSe_2$ are successfully applied to pulse lasers acting as saturable absorber (SA) in fiber laser and in waveguide laser, respectively [29,30]. $ReSe_2$, as a specific TMDs, is able to work as a SA. Because of the weak-layered dependent feature, it is not necessary to strictly control the thickness of $ReSe_2$ for many applications, which greatly simplifies the preparation requirements [17]. There is a report about a Q-switched fiber laser with $ReSe_2$ SA, whose shortest pulse width was 4.98 μs and highest repetition rate was 16.64 kHz [31]. However, based on $ReSe_2$ SA, the all-solid-state laser performances have not been reported.

In this paper, we firstly demonstrated a passively Q-switched Nd:YVO_4 laser incorporating $ReSe_2$ as SA in an all-solid-state laser. The $ReSe_2$ with a few-layer structure was prepared by the ultrasonic exfoliation technique. A series of measurements were used to characterize the properties of $ReSe_2$ sample. The saturation intensity was about 6.37 MW/cm^2, the non-saturable absorbance equaled to 16.84%, and the modulation depth was fitted to be 1.89%. For the Q-switched pulse laser, the threshold absorbed pump power was 227 mW. The maximum average output power was 125 mW. When the absorbed pump power was 837 mW, the shortest pulse width of 682 ns and the highest repetition rate of 84.16 kHz were obtained. Our experiment shows that the few-layer $ReSe_2$ could be used as 1 μm SA in all-solid-state lasers.

2. Preparation and Properties of Rhenium Diselenide

In the experiment, based on the feature of weak-layered dependence, there was no need to strictly control the uniformity of the $ReSe_2$ SA. So, the ultrasonic exfoliation method was chosen to prepare $ReSe_2$ SA. This method was simple and efficient. The $ReSe_2$ dispersion solution was prepared by adding 0.5 mg $ReSe_2$ powder to 200 mL of 15% alcohol. The mixture was placed in the ultrasonic cleaner for 48 h, and then stored at room temperature for 24 h. For the SA fabrication, the supernatant was made to spin on sapphire base and put in a drying cabinet for 24 h. Additionally, the properties of the $ReSe_2$ were characterized by using a Raman spectrometer (HORIBA LabRAM HR Evolution, Paris, France), a scanning electron microscope (SEM, Zeiss Sigma 500, Oberkochen, Germany), a transmission electron microscope (TEM, JEM-2100, Tokyo, Japan), and a home-built Yb-doped mode-locked laser.

Raman scattering experiments reported that $ReSe_2$ had the abundant spectra [16]. As shown in Figure 1a, the powdered $ReSe_2$ Raman spectrum is displayed. There were marked three main Raman shifts, corresponding to the E_g (124 cm^{-1}) and A_g (159 cm^{-1} and 173 cm^{-1}) modes. The E_g and A_g were equivalent to in-plane and out-of-plane vibrational modes, respectively. At the same time, because of the low-symmetry of $ReSe_2$, many small peaks were noticed in the experimental scope [32]. The morphology of $ReSe_2$ powder was elucidated by the SEM image, which is reproduced in Figure 1b. SEM image shows that the pre-dispersed $ReSe_2$ powder is a multi-layer structure with micro level in size.

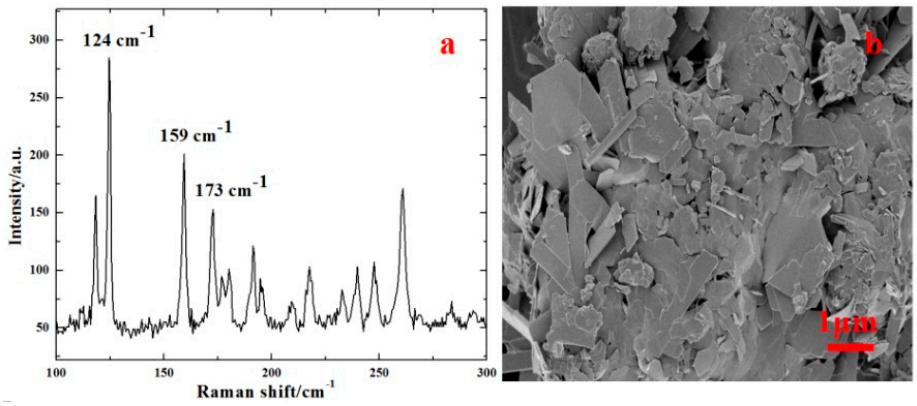

Figure 1. (**a**) Raman spectrum and (**b**) SEM image of $ReSe_2$ powder.

To test the shape of $ReSe_2$ through ultrasonic exfoliation, the TEM image of the dispersion solution is shown in Figure 2. Compared with the SEM image, $ReSe_2$ was effectively stripped into nano-scale sheets. The optical resolution of the TEM microscope was 50 nm.

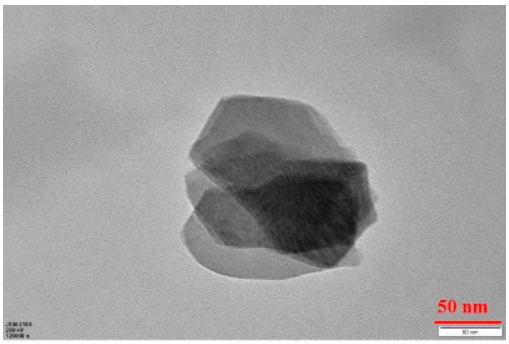

Figure 2. Transmission electron microscope (TEM) image of $ReSe_2$ dispersion solution.

A power-dependent transmission technique was employed for investigating the saturable absorption properties of $ReSe_2$ SA. For this experiment, the pump source was a home-built nonlinear polarization rotation mode-locked Yb-doped fiber laser with 68 ps pulse width at 1064 nm and repetition rate of 38.6 MHz. Based on the formula:

$$T(I) = 1 - T_{ns} - \Delta T \times \exp(-I/I_{sat}) \quad (1)$$

where $T(I)$ is the transmittance, T_{ns} represents the non-saturable absorbance, ΔT is the modulation depth, I signifies the input intensity of laser, and I_{sat} is the saturation intensity [30]. The experimental results are shown in Figure 3. Fitting the experimental results, the saturation intensity, non-saturable absorbance, and modulation depth were 6.37 MW/cm^2, 16.84%, and 1.89%, respectively. In subsequent experiments, attempts were made to change raw material parameters and optimize the preparation process. $ReSe_2$ SA materials with different parameters are expected to be obtained, thus making them more suitable for a variety of applications.

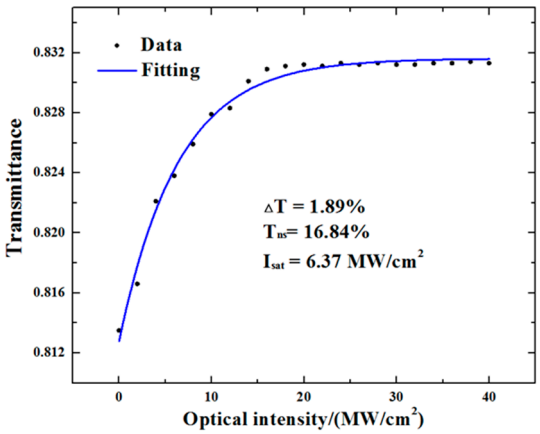

Figure 3. Nonlinear saturable absorption curve of the few-layer $ReSe_2$ SA.

3. The Passively Q-Switched Experiment

The passively Q-switched Nd:YVO_4 experiment was pumped by a fiber coupled diode laser. Its central wavelength, core diameter and numerical aperture were 808 nm, 200 μm and 0.22, respectively. An 1:1 optics coupling system focused the pump laser into a commercialized Nd:YVO_4 bulk crystal stabilized by a water-cooling system to remove heat. The linear type resonator had two mirrors, M1 and M2, of which M1 was the input mirror with radius of 100 mm and M2 was the output mirror with transmission of 5%. The cavity length was about 30 mm. After acquiring the continuous wave (CW) laser, the $ReSe_2$ SA was inserted in the resonator. Owing to the effect of $ReSe_2$ SA, the passively Q-switched laser was then obtained.

Figure 4a shows the average output power properties for CW and Q-switched laser. The CW laser obtained the maximum average output power of 284 mW and it had a slope efficiency of 36.72%. For the Q-switched laser, the threshold of absorbed pump power was 227 mW, and the pulse laser had an average output power of 17 mW. When the absorbed pump power was increased to 837 mW, the maximum average output power was 125 mW. The average output power was linear with the absorbed pump power, and the slope efficiency was 17.27%. As illustrated in the Figure 4b, the measured beam profile was close to the TEM_{00} mode, and the spot size is as shown. The laser spectrum, as shown in Figure 4c, is centered at 1064.4 nm, with a full width at half maximum of 0.68 nm (The spectrometer had a sampling resolution of 0.24 nm).

At the absorbed pump power of 227 mW, the passively Q-switched laser was established with a pulse width of 1.16 μs and repetition rate of 42.08 kHz. As the absorbed pump power increased, Figure 5a presents the behaviors of the pulse width and the pulse repetition rate. The experiment acquired the shortest pulse width of 682 ns and the highest repetition rate of 84.16 kHz. The corresponding pulse energy and peak power are shown in Figure 5b. Under the absorbed pump power of 837 mW, the Q-switched laser was calculated to be a pulse energy of 1.49 μJ and a pulse peak power of 2.18 W. Figure 6 shows the corresponding pulse form. For these measurements, we used a power meter (Ophir 30(150)A-BB-18, Jerusalem, Israel), optical spectrum analyzer (Ocean Optics HR4000, Largo, FL, USA), fast photodiode (EOT ET-3000A, Traverse, MI, USA), and digital oscilloscope (Tektronix MD03104, Beaverton, OR, USA).

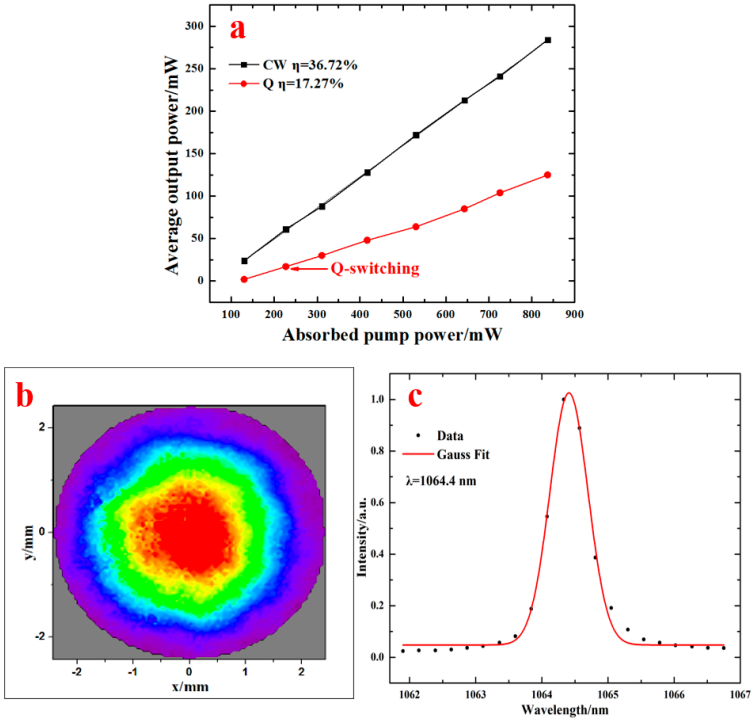

Figure 4. (**a**) Average output power properties for CW and Q-switched laser, (**b**) two-dimensional (2D) image of Q-switched output beam spatial profile, and (**c**) the laser spectrum at the maximum output power for Q-switching.

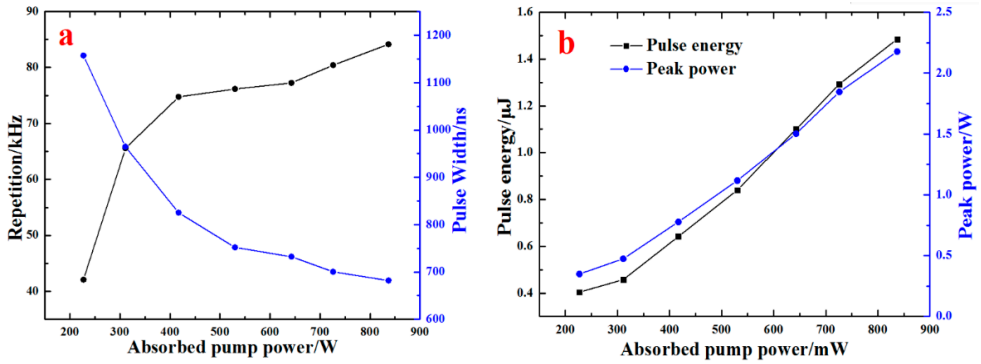

Figure 5. (**a**) The variation of the pulse width and repetition rate, and (**b**) the variation of the pulse energy and peak power.

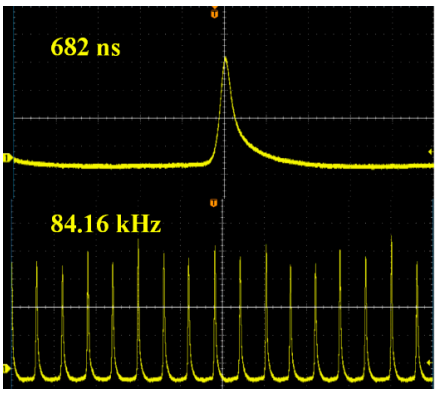

Figure 6. The pulse profile of the Q-switched laser.

Table 1 summarized the various Q-switched lasers that were used the diverse TMDs as SA in all-solid-state devices, with Nd-ion-doped gain medium and emitting wavelength at near 1064 nm. When compared with results, based on $ReSe_2$ SA, our works obtained the comparable laser performances. Table 1 concludes that $ReSe_2$ has the capacity to act as SA for all-solid-state pulse laser experiments. More importantly, the weaker interlayer coupling properties greatly reduced the preparation requirements of few-layer materials. Further optimizing the material, better results are expected to be achieved.

Table 1. Comparison of the passively Q-switched results in all-solid-state lasers based on transition metal dichalcogenides saturable absorber (TMDs SA).

Sa	Gain Medium	Pulse Width (ns)	Repetition Rate (kHz)	Output Power (mW)	Slope (%)	Ref.
MoS_2	Nd:LuAG	280	210	290	5.2	[33]
	Nd:YVO_4	327	5	199	9	[34]
	Nd:$GdVO_4$	970	732	227	-	[35]
	Nd:YAG	2800	20.8	23.5	-	[36]
WS_2	Nd:YVO_4	153	1578	1190	30	[37]
	Nd:$GdTaO_4$	560	70	309	6.87	[38]
		608	61.2	356	7.91	[38]
	Nd:YAG	922	52.48	42.6	-	[39]
		1030	47.05	46	-	[39]
		1280	45.25	54	-	[39]
$ReSe_2$	Nd:YVO_4	682	84.16	125	17.27	Our

4. Conclusions

In summary, a few-layer $ReSe_2$ was prepared by ultrasonic exfoliation and demonstrated as SA in an all-solid-state pulsed Nd:YVO_4 laser. The passively Q-switched Nd:YVO_4 experiment acquired the maximum average output power of 125 mW with a slope efficiency of 17.27%. The spectrum was centered at 1064.4 nm. The shortest pulse width was 682 ns and the highest repetition rate was 84.16 kHz, corresponding to a pulse energy of 1.49 μJ and pulse peak power of 2.18 W. Further, the $ReSe_2$ SA was characterized with its saturation intensity of 6.37 MW/cm^2 and modulation depth of 1.89%. The experiment results show that $ReSe_2$ is an effective SA for 1 μm all-solid-state pulse lasers and they promote the potential applications of weak-layered dependent TMDs.

Author Contributions: Y.L. supervised and supported the experiment. C.L. executed the experiments, handled the experimental data and wrote the manuscript. J.H. provided the $ReSe_2$ SA and corresponding parameters.

Funding: This research was funded by the Strategic Priority Research Program of the Chinese Academy of Sciences (Grant No. XDB1603); International S&T Cooperation Program of China (Grant No. 2016YFE0119300); National Natural Science Foundation of China (NSFC) (Grant Nos. 61521093, 61505234).

Conflicts of Interest: The authors declare no conflict of interest.

References

1. Bonaccorso, F.; Sun, Z.; Hasan, T.; Ferrari, A.C. Graphene photonics and optoelectronics. *Nat. Photonics* **2010**, *4*, 611–622. [CrossRef]
2. Wang, W.; Li, L.J.; Zhang, H.T.; Qin, J.P.; Lu, Y.; Xu, C.; Li, S.S.; Shen, Y.J.; Yang, W.L.; Yang, Y.Q.; Yu, X.Y. Passively Q-switched operation of a Tm, Ho:$LuVO_4$ laser with a graphene saturable absorber. *Appl. Sci.* **2018**, *8*, 954. [CrossRef]
3. Sobon, G. Mode-locking of fiber lasers using novel two-dimensional nanomaterials: Graphene and topological insulators. *Photonics Res.* **2015**, *3*, A56–A63. [CrossRef]
4. Wang, X.; Wang, Z.F.; Wang, Y.G.; Li, L.; Yang, G.W.; Li, J.P. Watt-level high-power passively Q-switched laser based on a black phosphorus solution saturable absorber. *Chin. Opt. Lett.* **2017**, *15*, 011402. [CrossRef]
5. Chen, H.; Yin, J.D.; Yang, J.W.; Zhang, X.J.; Liu, M.L.; Jiang, Z.K.; Wang, J.Z.; Sun, Z.P.; Guo, T.; Liu, W.J.; Yan, P.G. Transition-metal dichalcogenides heterostructure saturable absorbers for ultrafast photonics. *Opt. Lett.* **2017**, *42*, 4279–4282. [CrossRef] [PubMed]

6. Woodward, R.I.; Kelleher, E.J.R. 2D saturable absorbers for fibre lasers. *Appl. Sci.* **2015**, *5*, 1440–1456. [CrossRef]
7. Zhang, H.; Lu, S.B.; Zheng, J.; Du, J.; Wen, S.C.; Tang, D.Y.; Loh, K.P. Molybdenum disulfide (MoS_2) as a broadband saturable absorber for ultra-fast photonics. *Opt. Express* **2014**, *22*, 7249–7260. [CrossRef] [PubMed]
8. Woodward, R.I.; Howe, R.C.T.; Hu, G.; Torrisi, F.; Zhang, M.; Hasan, T.; Kelleher, E.J.R. Few-layer MoS_2 saturable absorbers for short-pulse laser technology: Current status and future perspectives. *Photonics Res.* **2015**, *3*, A30–A42. [CrossRef]
9. Janisch, C.; Mehta, N.; Ma, D.; Elías, A.L.; Perea-López, N.; Terrones, M.; Liu, Z.W. Ultrashort optical pulse characterization using WS_2 monolayers. *Opt. Lett.* **2014**, *39*, 383–385. [CrossRef] [PubMed]
10. Gonzalez, J.M.; Oleynik, I.I. Layer-dependent properties of SnS_2 and $SnSe_2$ two-dimensional materials. *Phys. Rev. B* **2016**, *94*, 125443. [CrossRef]
11. Huang, Y.; Sutter, E.; Sadowski, J.T.; Cotlet, M.; Monti, O.L.A.; Racke, D.A.; Neupane, M.R.; Wickramaratne, D.; Lake, R.K.; Parkinson, B.A.; Sutter, P. Tin disulfide; an emerging layered metal dichalcogenide semiconductor: Materials properties and device characteristics. *ACS Nano* **2014**, *8*, 10743–10755. [CrossRef] [PubMed]
12. Zhong, H.X.; Gao, S.Y.; Shi, J.J.; Yang, L. Quasiparticle band gaps, excitonic effects, and anisotropic optical properties of the monolayer distorted 1T diamond-chain structures ReS_2 and $ReSe_2$. *Phys. Rev. B* **2015**, *92*, 115438. [CrossRef]
13. Hafeez, M.; Gan, L.; Li, H.Q.; Ma, Y.; Zhai, T.Y. Chemical vapor deposition synthesis of ultrathin hexagonal $ReSe_2$ flakes for anisotropic Raman property and optoelectronic application. *Adv. Mater.* **2016**, *28*, 8296–8301. [CrossRef] [PubMed]
14. Su, X.C.; Nie, H.K.; Wang, Y.R.; Li, G.R.; Yan, B.Z.; Zhang, B.T.; Yang, K.J.; He, J.L. Few-layered ReS_2 as saturable absorber for 2.8 μm solid state laser. *Opt. Lett.* **2017**, *42*, 3502–3505. [CrossRef] [PubMed]
15. Zhang, E.Z.; Wang, P.; Li, Z.; Wang, H.F.; Song, C.Y.; Huang, C.; Chen, Z.G.; Yang, L.; Zhang, K.T.; Lu, S.H.; et al. Tunable ambipolar polarization-sensitive photodetectors based on high-anisotropy $ReSe_2$ nanosheets. *ACS Nano* **2016**, *10*, 8067–8077. [CrossRef] [PubMed]
16. Wolverson, D.; Crampin, S.; Kazemi, A.S.; Ilie, A.; Bending, S.J. Raman spectra of monolayer, few-layer, and bulk $ReSe_2$: An anisotropic layered semiconductor. *ACS Nano* **2014**, *8*, 11154–11164. [CrossRef] [PubMed]
17. Meng, M.; Shi, C.G.; Li, T.; Shi, S.E.; Li, T.H.; Liu, L.Z. Magnetism induced by cationic defect in monolayer $ReSe_2$ controlled by strain engineering. *Appl. Surf. Sci.* **2017**, *425*, 696–701. [CrossRef]
18. Tian, H.; Zhao, H.A.; Wang, H. Novel electronic and photonic properties of low-symmetry two-dimensional materials. In Proceedings of the 2016 IEEE International Conference on Electron Devices and Solid-State Circuits (EDSSC), Hong Kong, China, 3–5 August 2016; pp. 234–238.
19. Lorchat, E.; Froehlicher, G.; Berciaud, S. Splitting of interlayer shear modes and photon energy dependent anisotropic Raman response in N-layer $ReSe_2$ and ReS_2. *ACS Nano* **2016**, *10*, 2752–2760. [CrossRef] [PubMed]
20. Yang, S.X.; Wang, C.; Sahin, H.; Chen, H.; Li, Y.; Li, S.S.; Suslu, A.; Peeters, F.M.; Liu, Q.; Li, J.B.; Tongay, S. Tuning the optical, magnetic, and electrical properties of $ReSe_2$ by nanoscale strain engineering. *Nano Lett.* **2015**, *15*, 1660–1666. [CrossRef] [PubMed]
21. Cui, F.F.; Li, X.B.; Feng, Q.L.; Yin, J.B.; Zhou, L.; Liu, D.Y.; Liu, K.Q.; He, X.X.; Liang, X.; Liu, S.Z.; et al. Epitaxial growth of large-area and highly crystalline anisotropic $ReSe_2$ atomic layer. *Nano Res.* **2017**, *10*, 2732–2742. [CrossRef]
22. Qi, F.; Wang, X.Q.; Zheng, B.J.; Chen, Y.F.; Yu, B.; Zhou, J.H.; He, J.R.; Li, P.J.; Zhang, W.L.; Li, Y.R. Self-assembled chrysanthemum-like microspheres constructed by few-layer $ReSe_2$ nanosheets as a highly efficient and stable electrocatalyst for hydrogen evolution reaction. *Electrochim. Acta* **2017**, *224*, 593–599. [CrossRef]
23. Ho, C.H.; Huang, C.E. Optical property of the near band-edge transitions in rhenium disulfide and diselenide. *J. Alloy. Compd.* **2004**, *383*, 74–79. [CrossRef]
24. Ho, C.H.; Liao, P.C.; Huang, Y.S.; Yang, T.R.; Tiong, K.K. Optical Absorption of ReS_2 and $ReSe_2$ Single Crystals. *J. Appl. Phys.* **1997**, *81*, 6380–6383. [CrossRef]
25. Jian, Y.C.; Lin, D.Y.; Wu, J.S.; Huang, Y.S. Optical and electrical properties of Au- and Ag-doped $ReSe_2$. *Jpn. J. Appl. Phys.* **2013**, *52*, 04CH06. [CrossRef]
26. Ho, C.H.; Huang, Y.S.; Tiong, K.K.; Liao, P.C. Absorption-edge anisotropy in ReS_2 and $ReSe_2$ layered semiconductors. *Phys. Rev. B* **1998**, *58*, 16130–16135. [CrossRef]

27. Liu, H.; Luo, A.P.; Wang, F.Z.; Tang, R.; Liu, M.; Luo, Z.C.; Xu, W.C.; Zhao, C.J.; Zhang, H. Femtosecond pulse erbium-doped fiber laser by a few-layer MoS_2 saturable absorber. *Opt. Lett.* **2014**, *39*, 4591–4594. [CrossRef] [PubMed]
28. Lu, J.; Zou, X.; Li, C.; Li, W.K.; Liu, Z.Z.; Liu, Y.Q.; Leng, Y.X. Picosecond pulse generation in a mono-layer MoS_2 mode-locked Ytterbium-doped thin disk laser. *Chin. Opt. Lett.* **2017**, *15*, 041401.
29. Cheng, C.; Li, Z.Q.; Dong, N.N.; Wang, J.; Chen, F. Tin diselenide as a new saturable absorber for generation of laser pulses at 1 μm. *Opt. Express* **2017**, *25*, 6132–6140. [CrossRef] [PubMed]
30. Niu, K.D.; Chen, Q.Y.; Sun, R.Y.; Man, B.Y.; Zhang, H.N. Passively Q-switched erbium-doped fiber laser based on SnS_2 saturable absorber. *Opt. Mater. Express* **2017**, *7*, 3934–3943. [CrossRef]
31. Du, L.; Jiang, G.B.; Miao, L.L.; Huang, B.; Yi, J.; Zhao, C.J.; Wen, S.C. Few-layer rhenium diselenide: An ambient-stable nonlinear optical modulator. *Opt. Mater. Express* **2018**, *8*, 926–935. [CrossRef]
32. Jiang, S.L.; Zhang, Z.P.; Zhang, N.; Huan, Y.H.; Gong, Y.; Sun, M.X.; Shi, J.P.; Xie, C.Y.; Yang, P.F.; Fang, Q.Y.; et al. Application of chemical vapor–deposited monolayer $ReSe_2$ in the electrocatalytic hydrogen evolution reaction. *Nano Res.* **2018**, *11*, 1787–1797. [CrossRef]
33. Wang, C.; Zhao, S.Z.; Li, T.; Yang, K.J.; Luan, C.; Xu, X.D.; Xu, J. Passively Q-switched Nd:LuAG laser using few-layered MoS_2 as saturable absorber. *Opt. Commun.* **2018**, *406*, 249–253. [CrossRef]
34. Wang, G.J.; Song, Q.; Zhang, B.Y.; Gao, Y.J.; Wang, W.J.; Wang, M.H. Passively Q-switched Nd:YVO_4 laser using molybdenum disulfide (MoS_2) as a saturable absorber. *Optik-Int. J. Light Electron. Opt.* **2016**, *127*, 3021–3023. [CrossRef]
35. Wang, S.X.; Yu, H.H.; Zhang, H.J.; Wang, A.Z.; Zhao, M.W.; Chen, Y.X.; Mei, L.M.; Wang, J.Y. Broadband few-layer MoS_2 saturable absorbers. *Adv. Mater.* **2014**, *26*, 3538–3544. [CrossRef] [PubMed]
36. Lin, T.; Sun, H.; Wang, X.; Mao, D.; Wang, Y.G.; Li, L.; Duan, L.N. Passively Q-switched Nd:YAG laser with a MoS_2 solution saturable absorber. *Laser Phys.* **2015**, *25*, 125805. [CrossRef]
37. Wang, X.; Li, L.; Li, J.P.; Wang, Y.G. 1.5-MHz repetition rate passively Q-switched Nd:YVO_4 laser based on WS_2 saturable absorber. *Chin. Phys. B* **2017**, *26*, 044203. [CrossRef]
38. Li, M.X.; Jin, G.Y.; Li, Y. Diode-pumped passively Q-switched Nd:$GdTaO_4$ laser based on tungsten disulfide nanosheets saturable absorber at 1066 nm. *Infrared Phys. Techn.* **2018**, *90*, 195–198. [CrossRef]
39. Wang, X.; Wang, Y.G.; Duan, L.N.; Li, L.; Sun, H. Passively Q-switched nd:YAG laser via a WS_2 saturable absorber. *Opt. Commun.* **2016**, *367*, 234–238. [CrossRef]

© 2018 by the authors. Licensee MDPI, Basel, Switzerland. This article is an open access article distributed under the terms and conditions of the Creative Commons Attribution (CC BY) license (http://creativecommons.org/licenses/by/4.0/).